Development 133, 1183-1192 (2006) doi:10.1242/dev.02293

Roles for Dnmt3b in mammalian development: a mouse model for the ICF syndrome

Yoshihide Ueda[1], Masaki Okano[1,3], Christine Williams[2], Taiping Chen[1,4], Katia Georgopoulos[2] and En Li[1,4,*]

ICF (Immunodeficiency, Centromeric instability and Facial anomalies) syndrome is a rare autosomal recessive disease caused by mutations in the DNA methyltransferase gene *DNMT3B*. To investigate the function of Dnmt3b in mouse development and to create animal models for ICF syndrome, we have generated three mutant alleles of *Dnmt3b* in mice: one carrying a deletion of the catalytic domain (null allele) and two carrying ICF-like missense mutations in the catalytic domain. The *Dnmt3b* null allele results in embryonic lethality from E14.5 to E16.5 with multiple tissue defects, including liver hypotrophy, ventricular septal defect and haemorrhage. By contrast, mice homozygous for the ICF mutations develop to term and some survive to adulthood. These mice show phenotypes that are reminiscent of ICF patients, including hypomethylation of repetitive sequences, low body weight, distinct cranial facial anomalies and T cell death by apoptosis. These results indicate that Dnmt3b plays an essential role at different stages of mouse development, and that ICF missense mutations cause partial loss of function. These mutant mice will be useful for further elucidation of the pathogenic and molecular mechanisms underlying ICF syndrome.

KEY WORDS: DNA methylation, Dnmt3b, ICF syndrome, T cell, Apoptosis

INTRODUCTION

ICF syndrome is a rare autosomal recessive disorder characterized by immunodeficiency, centromeric instability and facial anomalies (Ehrlich, 2003; Wijmenga et al., 2000). Individuals with this disease show combined immunodeficiency, including absence or severe reduction of at least two classes of immunoglobulin and a reduced number of T cells, making them prone to infections and death before adulthood. Centromeric instability is characterized by the formation of radiated chromosomes (chromosome 1, 9 and 16) due to demethylation at cytosine residues in classical satellites 2 and 3 at juxtacentromeric regions of these chromosomes. Facial anomalies include hypertelorism, flat nasal bridge, low set ears, protrusion of the tongue, epicanthal folds, micrognathia and high forehead. Most individuals also exhibit growth and mental retardation. Several studies have demonstrated that ICF syndrome is caused by homozygous or compound heterozygous mutations of the DNA methyltransferase 3B (*DNMT3B*) gene (Hansen et al., 1999; Okano et al., 1999; Xu et al., 1999).

Dnmt3b is one of the three active DNA cytosine methyltransferases identified in human and mouse (Okano et al., 1998; Xie et al., 1999). Dnmt3a and Dnmt3b have high structural similarity, and both can carry out de novo methylation in embryonic stem cells and during embryonic development (Okano et al., 1999). Although these two enzymes exhibit overlapping functions during early development, each has distinct expression patterns, genomic targets and functions (Chen et al., 2003; Okano et al., 1999). Although *Dnmt3a* deficient mice develop to term and appear to be normal at birth, *Dnmt3b* deficient mice are embryonic lethal. Recently, Dnmt3a, but not Dnmt3b, has been shown to be essential for the establishment of methylation imprints during gametogenesis (Kaneda et al., 2004). Genetic analysis of *Dnmt3a* and *Dnmt3b* function in embryonic stem cells has revealed that Dnmt3a and Dnmt3b, and their different variants, have shared as well as distinct DNA targets (Chen et al., 2003). However, the specific functions of Dnmt3a or Dnmt3b in vivo have not been fully analyzed yet.

To investigate the function of Dnmt3b in mouse development and to determine whether *Dnmt3b* mutations result in phenotypes similar to those of individuals with ICF syndrome, we generated mice with point mutations in *Dnmt3b* corresponding to the mutations found in human patients (ICF mice). Our studies of *Dnmt3b* null and ICF mutant mice show that Dnmt3b is essential for mouse embryonic development, and that the ICF mice exhibit phenotypes that resemble some of the symptoms of the human ICF syndrome. We also demonstrate that Dnmt3b is essential for the survival of T cells in the thymus of newborn mice.

MATERIALS AND METHODS

Vectors

Construction of the GFP-Dnmt3b1, GFP-Dnmt3b2, GFP-Dnmt3b3, myc-Dnmt3a and myc-Dnmt3b1 vectors has been described previously (Chen et al., 2002; Hata et al., 2002). Human *DNMT3B* cDNA was synthesized by RT-PCR from total RNA of NT-2 cells, by using the oligonucleotides 5′-ATGAAGGGAGACACCAGGC-3′ and 5′-GCCTGGCTGGAACTATTCAC-3′ as primers, and subcloned into pCAG-IRESblast vector. The cDNAs of ICF mutants were generated by a PCR-based site-directed mutagenesis experiment, by using mouse *Dnmt3b1* or human *DNMT3B* cDNA as template, and subcloned into the pEGFP-C1 (CLONTECH) and/or the pCAG-IRESblast vector. The *Dnmt3b* A609T and D823G knock-in vectors were generated by sequentially subcloning *Dnmt3b* fragments and a floxed IRES-βgeo cassette, in which IRES-βgeo is flanked by loxP sites, into pBluescript II SK. The fragments containing A609T and D823G mutations were generated by PCR using a bacterial artificial chromosome clone as a template and the following oligonucleotides as primers: 5′-CTGGAGCTGCTATATGTGCC-3′, 5′-GGAAAAGTACATTACCTCCGA-3′, 5′-CACAGACTTCGGAGGTAATG-3′ and 5′-TTGGTGATTTTCCGGACGTC-3′ for A609T; and 5′-CAGACAGGGCAAAAACCAGC-3′ and 5′-CCGCGGCCCATGTTGGACACGCC-3′ for D823G. The other *Dnmt3b* fragments were obtained from a bacterial artificial chromosome clone. The identities of all constructs were verified by DNA sequencing.

[1]Cardiovascular Research Center, Massachusetts General Hospital, Harvard Medical School, 149 13th Street, Charlestown, MA 02129, USA. [2]Cutaneous Biology Research Center, Massachusetts General Hospital, Harvard Medical School, 149 13th Street, Charlestown, MA 02129, USA. [3]Center for Developmental Biology, RIKEN, Kobe Hyogo 650-0047, Japan. [4]Epigenetics Program, Novartis Institutes for Biomedical Research, 250 Massachusetts Avenue, Cambridge, MA 02139, USA.

*Author for correspondence (e-mail: en.li@pharma.novartis.com)

Accepted 18 January 2006

Protein expression and analysis

Transient transfection was carried out in COS-7 cells for immunoprecipitation assay and NIH3T3 cells for fluorescence microscopy analysis, using LipofectAMINE PLUS reagent (Invitrogen). Immunoprecipitation, immunoblotting and fluorescence microscopy analyses were performed as previously described (Chen et al., 2002; Hata et al., 2002). Stable transfection of *Dnmt3b*-expression vectors in ES cells was performed according to a procedure described previously (Chen et al., 2003). The antibodies used in these experiments were anti-myc (Roche), anti-GFP (Roche), anti-Dnmt3b, anti-Dnmt3a (clone 64B1446; Imgenex), and anti-α-tubulin (Ab-1; Oncogene Research Products).

Generation of ICF mutant mice

The *Dnmt3b* A609T and D823G targeting vectors were transfected into ES cells via electroporation, and transfected cells were selected with G418, as previously described (Li et al., 1992). Clones with homologous recombination were identified by Southern blot analysis. Genomic DNA from ES cell clones was digested with *Bam*HI, blotted and hybridized to an external probe. The wild-type, null, A609T and D823G alleles give fragments of 17 kb, 5.7 kb, 6.5 kb, and 14 kb, respectively (Fig. 2D). Chimeric mice and F1 heterozygotes were generated from multiple A609T or D823G mutant ES cell lines as described (Li et al., 1992). Mutant mice were maintained on a 129SvJae×C57BL/6 hybrid background and analyzed.

DNA methylation analysis

Genomic DNA isolated from ES cells, E12.5 embryos, tissues of newborns, and tails of adult mice was digested with methylation-sensitive restriction enzymes and analyzed by Southern hybridization as previously described (Chen et al., 2003; Lei et al., 1996). The probes used for methylation analysis were: pMR150 for minor satellite repeats, pMO for endogenous C-type retroviruses, and an oligonucleotide probe for major satellite repeats.

Histological analysis, TUNEL assay, and skeletal staining

For histological analysis and TUNEL assay, tissues were fixed in 10% buffered formalin and processed into paraffin wax-embedded sections using routine procedures. For general morphology, deparaffinized sections were stained with Hematoxylin and Eosin using standard procedures. TUNEL assay was performed using the ApopTag Plus Fluorescein In Situ Apoptosis Detection Kit (Serologicals Corporation), by following the manufacturer's protocol. For skeletal staining, mice were skinned, placed in 1.5% KOH and macerated. After 4-5 days, the mice were stained in Alizarin Red for 3 days, and then placed in 1.5% KOH for 1 day to remove the excess stain. The stained bones were then transferred to glycerol.

Flow cytometric analysis

Cells from the thymus, spleen, and bone marrow were prepared and analyzed for the expression of surface differentiation antigens as described (Georgopoulos et al., 1994; Winandy et al., 1995). Flow cytometric analysis was performed using a FACScan flow cytometer (BD). All antibodies used for staining were from PharMingen.

RESULTS

ICF mutations result in loss of function via disrupting protein-protein interactions and/or by perturbing protein localization

To address how the ICF mutations affect Dnmt3b function, we introduced six ICF mutations into mouse *Dnmt3b* cDNA (Fig. 1A) in expression vectors. A609T, L670T, V732G, A772P and D823G are missense mutations corresponding to the human ICF mutations A603T, L664T, V726G, A766P and D817G, respectively (Okano et al., 1999; Wijmenga et al., 2000; Xu et al., 1999). STP813ins is a 9 bp insertion at codon 813 encoding three amino acids, serine, threonine and proline, corresponding to the change found in a patient with ICF syndrome (Okano et al., 1999).

First, the ability of Dnmt3b mutant proteins to interact with Dnmt3a was examined. Immunoprecipitation analysis was performed using GFP-Dnmt3b fusion proteins and myc-tagged Dnmt3a (Fig. 1B). As previously reported, Dnmt3b1 was co-immunoprecipitated with Dnmt3a, as well as with Dnmt3b1 itself (Kim et al., 2002). We also showed the binding of endogenous Dnmt3a to endogenous Dnmt3b in ES cells by co-immunoprecipitation assay (see Fig. S1 in the supplementary material). The A609T mutation disrupted the interaction with Dnmt3a, as well as with Dnmt3b1. The other ICF mutations did not affect this interaction. Further mutagenesis analysis revealed that the region of Dnmt3b required for its interaction with Dnmt3a is in the amino-terminal region of the catalytic domain, including alanine 609 (see Fig. S1 in the supplementary material), suggesting that the A609T mutation alters the conformation of the Dnmt3a interaction domain.

We next examined the subcellular localization of these mutant proteins using GFP fusion proteins. As described before (Bachman et al., 2001; Chen et al., 2004), wild-type Dnmt3b1 and Dnmt3b2 displayed punctate nuclear localization patterns with two major types of nuclear foci: large foci, which corresponded to pericentric heterochromatin; and small foci, which were distributed throughout the nucleus, excluding the nucleoli. Both types of foci were present in the majority of transfected cells (pattern A); however, only the small foci were visible in some transfected cells (pattern B). By contrast, Dnmt3b3, which lacks part of motif IX in the catalytic domain and has no enzymatic activity, displayed diffuse nuclear localization patterns with or without accumulation in pericentric heterochromatin (patterns C and D, respectively). Four of the ICF mutations, A609T, V732G, STP813 and D823G, exhibited obvious changes in localization patterns when compared with wild-type Dnmt3b1. A609T showed no accumulation in pericentric heterochromatin (~75% of transfected cells showed pattern B and the rest showed pattern D), suggesting that Dnmt3a-Dnmt3b heterodimerization and/or Dnmt3b homodimerization may be required for targeting Dnmt3b to pericentric heterochromatin. V732G, STP813 and D823G showed diffuse patterns similar to those of Dnmt3b3, indicating that these mutations disrupt the association of Dnmt3b with the small type of nuclear foci. Although the identity of these foci remains to be determined, it is possible that these structures correspond to heterochromatin regions, which usually consist of repetitive DNA sequences, including satellite repeats. Failure to target Dnmt3b to heterochromatin may thus contribute to demethylation of satellite DNA, a hallmark of ICF syndrome. The other two mutations, L670T and A772P, did not affect the localization patterns of Dnmt3b, although a minor increase in the number of cells exhibiting pattern B was observed with the L670T mutation (Fig. 1C).

We then examined the effects of the ICF mutations on the methyltransferase activity of Dnmt3b. Mouse *Dnmt3b1*, A609T, D823G and PC (*Dnmt3b1* with its PC motif mutated), as well as human *DNMT3B1*, A603T and D817G, cDNAs were introduced into highly demethylated *Dnmt3a*$^{-/-}$*Dnmt3b*$^{-/-}$ ES cells. Individual clones that expressed different levels of these proteins, as determined by immunoblotting analysis, were obtained (Fig. 1D). DNA methylation patterns were examined using genomic DNA isolated from these clones. As reported previously (Chen et al., 2003), expression of wild-type Dnmt3b1 substantially restored the methylation levels of all the repetitive sequences examined. We found that human DNMT3B1 could also restore the methylation levels of the mouse endogenous C-type retroviral DNA (Fig. 1E), and of the major and minor satellite repeats (data not shown). By contrast, mouse A609T and D823G, as

well as human A603T and D817G, proteins failed to restore the DNA methylation of these repetitive sequences, suggesting that these ICF mutants have little or no methyltransferase activity.

Taken together, our results suggest that different ICF mutations result in a loss of function via different mechanisms; some by disrupting protein-protein interactions and others by altering protein localization.

Generation of mouse models for ICF syndrome

Two ICF mutations, A609T, which disrupts the interactions with Dnmt3a and Dnmt3b1, and D823G, which alters protein localization, were introduced into the mouse *Dnmt3b* gene by homologous recombination, using a loxP-flanked IRES-βgeo cassette as a selection marker (Fig. 2A). The IRES-βgeo cassette was removed by crossing the heterozygous mice with EIIa-Cre that expresses Cre recombinase

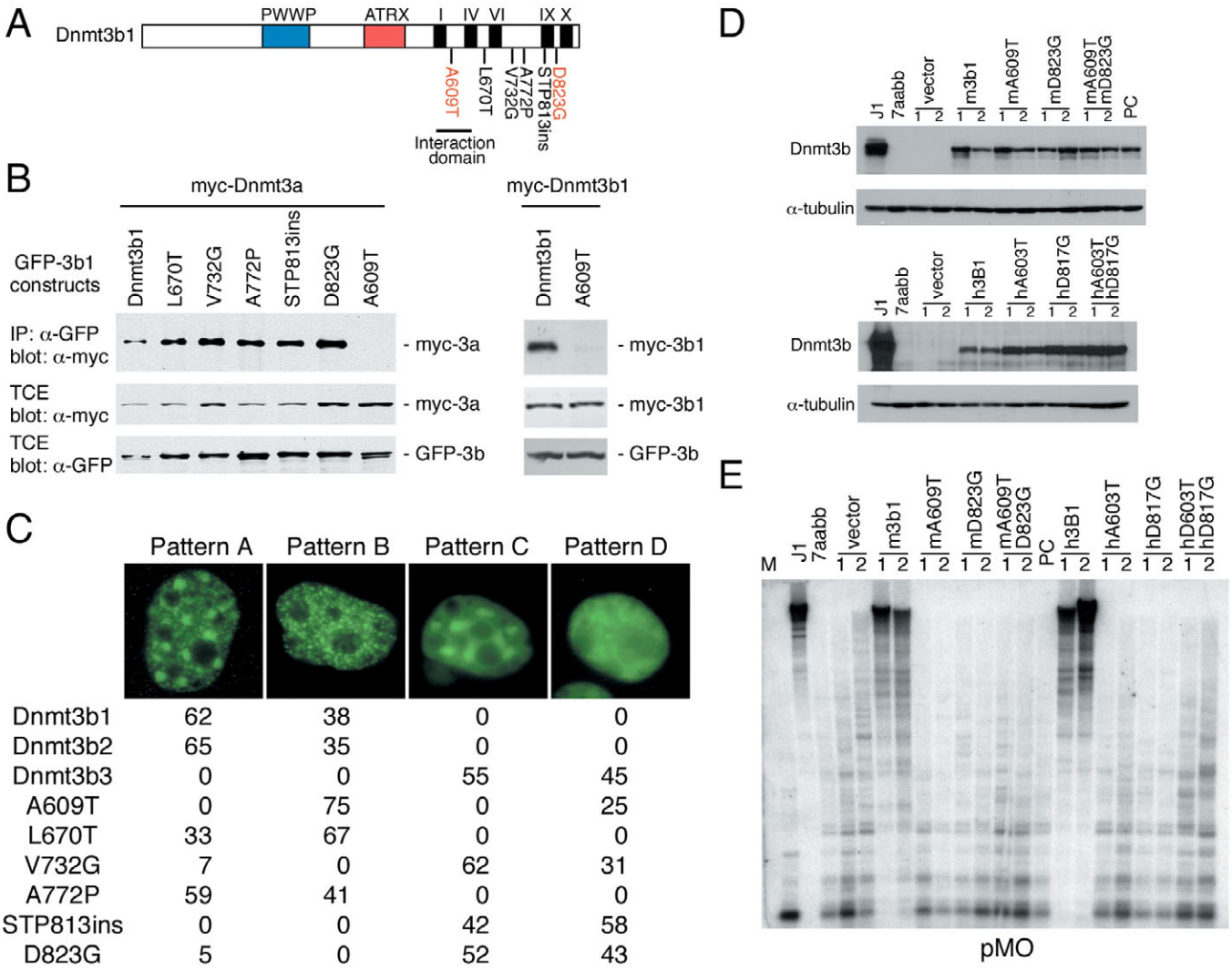

Fig. 1. Biochemical characterization of ICF mutations. (**A**) Schematic diagram of the mouse Dnmt3b protein structure. The conserved PWWP and ATRX domains, the methyltransferase motifs (I, IV, VI, IX and X), and the ICF mutations that we introduced into mouse *Dnmt3b* cDNA are indicated. The location of the interaction domain with Dnmt3a (see Fig. S1 in the supplementary material) is also shown. (**B**) Interaction of ICF mutants with wild-type Dnmt3a and Dnmt3b. COS-7 cells were transfected with two expression vectors, one for myc-Dnmt3a (left panel) or myc-Dnmt3b1 (right panel), and another for GFP-Dnmt3b1 or GFP-ICF mutants, as indicated. GFP-tagged proteins were immunoprecipitated from cell extracts using an anti-GFP antibody. Immunoblotting analysis of the immunoprecipitates was carried out using anti-myc antibody (top panel). The middle and bottom panels show the results of immunoblotting of the total cell extract (TCE) from transfected cells with anti-myc and anti-GFP antibodies, respectively. (**C**) Subcellular localization of Dnmt3b isoforms and ICF mutants. GFP-tagged Dnmt3b isoforms or ICF mutants were expressed in NIH3T3 cells, and the cells were fixed and analyzed by fluorescence microscopy. For each construct, 200-300 transfected (green) cells were counted and the percentages of cells showing different localization patterns are indicated. (**D**) Stable expression of wild-type and mutant Dnmt3b in *Dnmt3a*$^{-/-}$, *Dnmt3b*$^{-/-}$ ES cells. Expression vectors encoding mouse Dnmt3b1 (m3b1), A609T, D823G and PC (Dnmt3b with its PC motif mutated) (top panel), and human DNMT3B (h3B1), A603T and D817G (lower panel), were individually (or in a combination of two ICF mutants) electroporated into late-passage 7aabb cells and selected in blasticidin-containing medium. Blasticidin-resistant clones were analyzed by immunoblotting using anti-Dnmt3b and anti-α-tubulin antibodies. (**E**) DNA methylation analysis. Genomic DNA from the indicated ES cell lines was digested with *Hpa*II and analyzed by Southern hybridization using a probe (pMO) for the endogenous C-type retrovirus repeats. DNA from wild-type ES cells (J1) digested with *Msp*I (M) was used as a control for complete digestion.

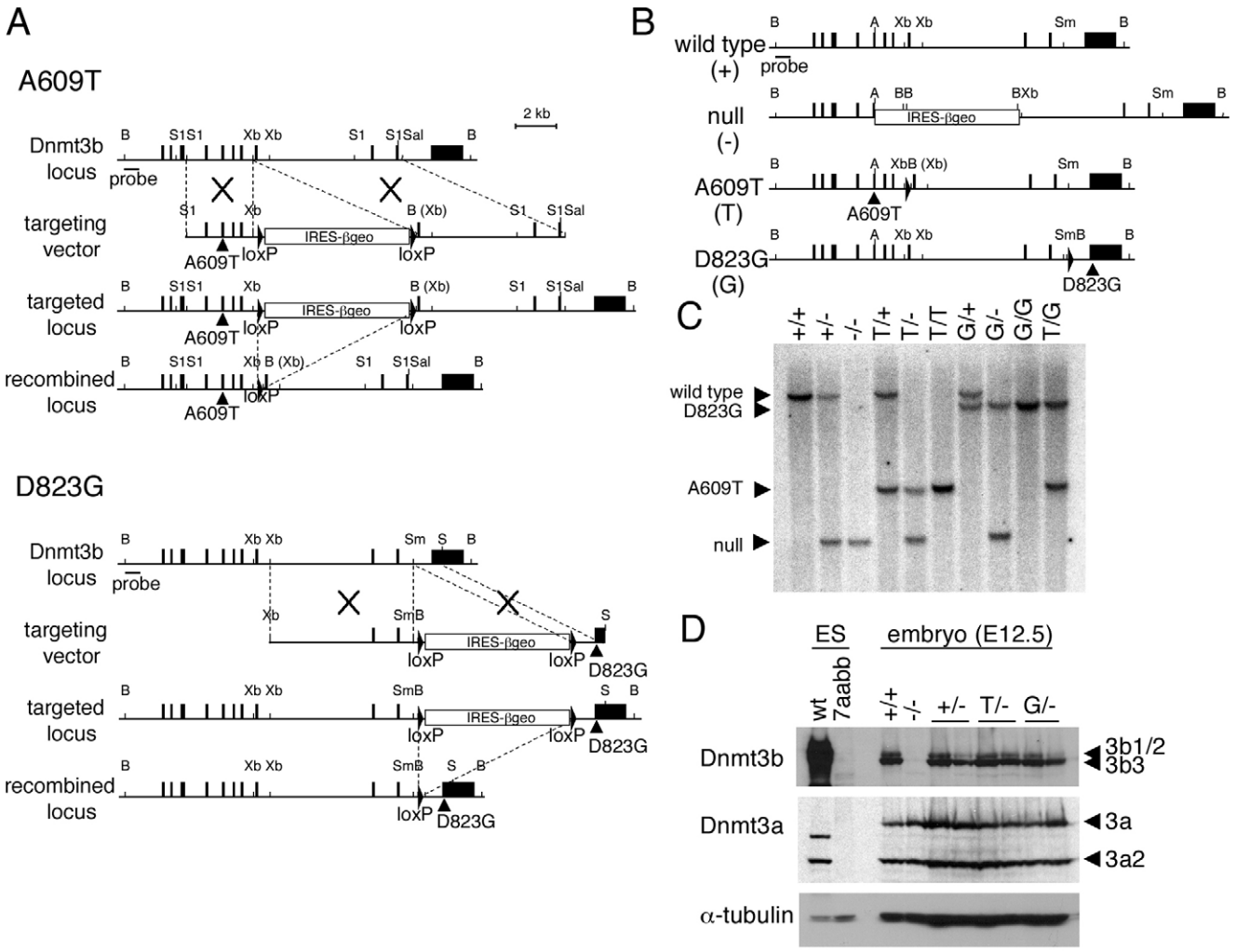

Fig. 2. Generation of mouse models for ICF syndrome. (**A**) Maps of the *Dnmt3b* genomic locus, targeting vector, targeted locus, and recombined locus after exposure to Cre. The vertical bars represent the exons; arrowheads indicate the ICF mutations introduced. B, *Bam*HI; E5, *Eco*RV; S1, *Sac*I; Xb, *Xba*I; Sal, *Sal*I; Sm, *Sma*I. (**B**) Maps of *Dnmt3b* wild-type and mutant (n=3) alleles used in this study. (**C**) Southern blot analysis of the different *Dnmt3b* alleles. Genomic DNA was digested with *Bam*HI and hybridized with a 5′ external probe indicated in A and B. (**D**) Immunoblot analysis of protein samples prepared from whole E12.5 embryos and ES cells with anti-Dnmt3b (upper panel), anti-Dnmt3a (middle panel) and anti-α-tubulin (lower panel) antibodies. The migration of Dnmt3a and Dnmt3b isoforms is indicated (arrowheads).

in the unfertilised egg of the female germline (Lakso et al., 1996). We have previously generated a *Dnmt3b* null allele in which the region of the catalytic domain that encompassed the highly conserved PC and ENV motifs was deleted (Okano et al., 1999). The three different mutant alleles of *Dnmt3b* are shown in Fig. 2B. These alleles could be distinguished by Southern blot analysis (Fig. 2C), and the point mutations were confirmed by sequence analysis of genomic DNA extracted from the tails of the heterozygous mice (data not shown). Mice carrying A609T and D823G mutations produced full-length proteins at levels similar to those of wild-type mice, whereas no Dnmt3b protein was detected in *Dnmt3b*$^{-/-}$ mice, as determined by immunoblotting of E12.5 embryo extracts with Dnmt3b antibody (Fig. 2D). The expression of Dnmt3a and Dnmt3a2 proteins was not affected by the *Dnmt3b* mutations (Fig. 2D). We tried to confirm the effects of the A609T and D823G mutations on Dnmt3b subcellular localization in vivo. Immunostaining of wild-type and mutant embryos at E8.5 and E12.5, as well as of wild-type embryonic fibroblasts, only detected weak signals of a diffuse nuclear pattern (data not shown), consistent with the observations that the level of Dnmt3b is low (as compared with that in ES cells) and that the major isoform is Dnmt3b3 at these developmental stages (Fig. 2D).

ICF mutations result in a partial loss of function of Dnmt3b

Mice heterozygous for the *Dnmt3b* A609T, D823G or null mutation appeared to be grossly normal, fertile and indistinguishable from their wild-type littermates. As reported previously, *Dnmt3b*$^{-/-}$ mice are embryonic lethal (Okano et al., 1999), so no homozygous newborn mice were found (Fig. 3A). By contrast, normal Mendelian frequencies of mice with T/–, G/–, T/T, G/G and T/G genotypes were found at birth, but most of the mutant mice died within 24 hours after birth. A few mice survived longer than 24 hours, and only four mice (three T/T mice and one T/G mice) were found at weaning age (about 3 weeks). These differences in lethality between *Dnmt3b*$^{-/-}$ and the ICF mutants indicate that the ICF mutations are not complete loss-of-function alleles.

A

+/- x +/-

	+/+	+/-	-/-
newborn	15	37	0

T/+ x +/-

	+/+	+/-	T/+	T/-
3 weeks	76	74	73	0
newborn	17	16	9	13

G/+ x +/-

	+/+	+/-	G/+	G/-
3 weeks	29	33	40	0
newborn	13	11	19	11

T/+ x T/+

	+/+	T/+	T/T
3 weeks	40	62	3
newborn	17	31	13

G/+ x G/+

	+/+	G/+	G/G
3 weeks	35	68	0
newborn	17	29	11

T/+ x G/+

	+/+	T/+	G/+	T/G
3 weeks	38	36	33	1
newborn	18	14	14	14

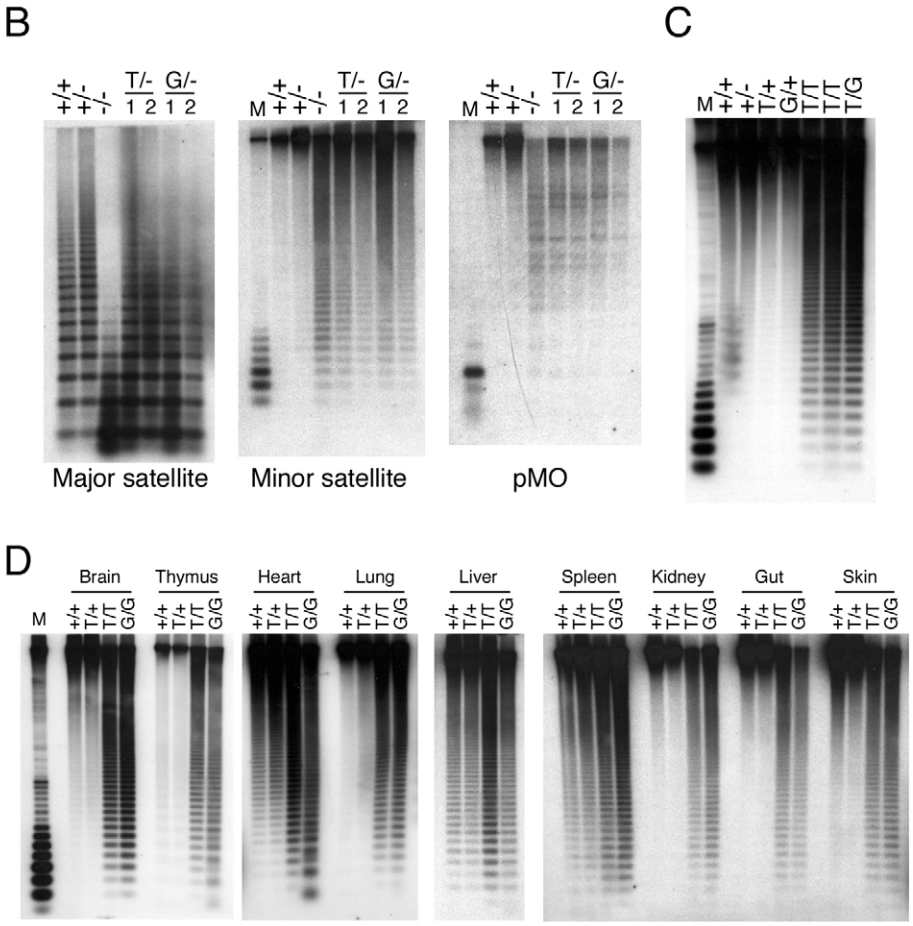

Fig. 3. ICF mutations result in a partial loss of function of Dnmt3b. (**A**) Progeny derived from intercrosses of *Dnmt3b* mutants. (**B-D**) DNA methylation analysis of *Dnmt3b* mutant mice. Genomic DNA from E12.5 embryos (B), tails of adult mice (C) and various tissues of newborns (D) was digested with *Hpa*II or *Mae*II (left panel of B) and hybridized to probes for major satellite repeats (left panel of B), minor satellite repeats (middle panel of B;C,D), and endogenous C-type retrovirus repeats (pMO; right panel of B). DNA digested with *Msp*I (M) was used as a control for a complete lack of DNA methylation.

To determine whether the ICF mutations in *Dnmt3b* affected global methylation of genomic DNA, we examined the methylation status of three repetitive sequences: major satellite repeats, minor satellite repeats and C-type retrovirus. We found that these repeats were demethylated in *Dnmt3b* mutant embryos, and in newborn and adult mice. DNA methylation levels in ICF mutant mice were significantly higher than in *Dnmt3b*$^{-/-}$ mice, confirming that the ICF mutations resulted in a partial loss of function of Dnmt3b. No difference between A609T and D823G was detected (Fig. 3B-D). Hypomethylation was observed in all tissues that we tested in newborn mice (Fig. 3D), although the expression of Dnmt3b is regulated during embryogenesis and restricted in some tissues at later stages. Moreover, DNA in adult ICF mice was hypomethylated to a similar extent as that in embryos and newborns (Fig. 3C).

The *Dnmt3b* null mutation results in embryonic lethality with multiple tissue defects

To investigate the role of Dnmt3b in mouse development, we first analyzed *Dnmt3b*$^{-/-}$ embryos. Dissection of embryos revealed that most of the *Dnmt3b*$^{-/-}$ mice were lethal between 13.5 days post-coitum (dpc) and 16.5 dpc (Fig. 4A), showing progressive necrosis. All of the live *Dnmt3b*$^{-/-}$ embryos that were recovered at this stage showed subcutaneous edema and liver atrophy (Fig. 4B,C,F), which became apparent at 13.5 dpc. Some of the *Dnmt3b*$^{-/-}$ embryos showed ectopic hemorrhage in the head region (Fig. 4B). Furthermore, genotyping revealed that *Dnmt3b*$^{-/-}$ embryos were slightly underrepresented from the expected Mendelian ratio at 11.5-13.5 dpc [Fig. 4A, *Dnmt3b*$^{+/+}$:*Dnmt3b*$^{+/-}$:*Dnmt3b*$^{-/-}$ = 57(27%): 100(48%): 33(14%)], suggesting an earlier lethality of *Dnmt3b*$^{-/-}$ embryos in a small population (about 30%). Occasionally, we recovered abnormal *Dnmt3b*$^{-/-}$ embryos between 9.5 and 12.5 dpc (Okano et al., 1999), but the cause of lethality was unclear.

Serial sections of the thoracic region of *Dnmt3b*$^{-/-}$ embryos revealed that the ventricular septum was not closed in the heart of *Dnmt3b*$^{-/-}$ embryos at 14.5 and 15.5 dpc (Fig. 4D, and data not shown), although ventricular septum closure is normally completed by 13.5 dpc in mice (Webb et al., 1998). Other histological features of the heart, such as trabeculation, were normal in *Dnmt3b*$^{-/-}$ embryos. We also found hemorrhaging in the middle of the dorsal root ganglia and in the limb region (Fig. 4E, and data not shown), which suggests defects of blood vessel formation or maintenance in *Dnmt3b*$^{-/-}$ embryos. We hypothesize that the ventricular septum defect and blood vessel abnormalities account for the subcutaneous edema of *Dnmt3b*$^{-/-}$ embryos.

The fetal liver of *Dnmt3b*$^{-/-}$ embryos was much smaller (about one fifth) than that of normal littermates (Fig. 4F). Because the fetal liver is a major hematopoietic organ at this stage, we examined expression of the late erythroid marker TER-119 and the hepatocyte marker albumin in the liver of *Dnmt3b*$^{-/-}$ embryos by immunohistochemistry (data not shown). However, we did not see a dramatic change in the erythroblast or hepatocyte populations, suggesting that a defect in hematopoiesis was not the sole reason for this phenotype. We also did not observe significant differences in BrdU incorporation or TUNEL staining in the mutant fetal liver (data not shown), suggesting that the proliferation and apoptosis of hepatocytes was normal.

Mice with ICF mutations develop to term

In contrast to *Dnmt3b*$^{-/-}$ animals, mice with ICF mutations (T/T, G/G, T/G, T/– and G/–) developed to term and were alive at birth. These mice showed no sign of edema or liver atrophy, although some exhibited hemorrhage in the head region. The gross anatomy of the mutant mice appeared to be normal, although the body size of the mutant mice was much smaller than that of the control mice (Fig. 5A,B). The body weight of the mutant mice was less than two-thirds of that of the normal littermates at birth, and the adult mutant mice that survived remained smaller (Fig. 5C).

All four types of adult ICF mice showed characteristic facial anomalies, such as shorter nose and wider nasal bridge, as shown in Fig. 5D. These features are similar to the hypertelorism and the flat nasal bridge that are frequently seen in individuals with ICF syndrome. The craniofacial defects were further characterized after skeletal preparations were made (Fig. 5E). The calvarium of adult T/T mice showed abnormally shaped frontal bones. The frontal bones of ICF mice were wider than those of normal littermates, resulting in a wider distance between the eyes. The lateral view revealed that the frontal and parietal bones were round shaped (data not shown). The nasal bone of T/T mice was significantly shorter, whereas the axial length of the calvarium of the mutant mice was the same as that of the control mice. The skeletons of newborn ICF mice showed a similar defect to that of the adults (Fig. 5F). An enlarged frontal fontanel was present in the mutant, indicating that ossification was delayed at the newborn stage. These craniofacial defects were observed in all newborn and adult mice that had T/T, G/G, T/G, T/– or G/– mutations.

Dnmt3b mutations lead to apoptosis of thymocytes

To investigate whether *Dnmt3b* mutant mice had immune defects as seen in human ICF patients, the bone marrow and thymus of the newborn mice were analyzed. B cell populations in the bone marrow of ICF mice (P0-P1) were analyzed by flow cytometric analysis using anti-B220 and anti-IgM antibodies. No significant differences in these precursor and mature B cell populations were observed between ICF mice and littermate controls (data not shown). The thymus of ICF mice was then examined for T cell developmental defects. The number of thymocytes in newborn (P0) ICF mice was similar to that of their littermate controls, and flow cytometric analysis of CD4, CD8 and TCRβ expression revealed no developmental defects in the thymus (data not shown), suggesting that mutations in *Dnmt3b* do not affect the development of T cells. The thymuses of P1 ICF mice (born 24 to 48 hours before analysis)

A

Dnmt3b+/- X Dnmt3b+/-

Stage (dpc)	Total	+/+	+/-	-/-	N.D.
16.5	72	11	40	5 (5)	16
15.5	36	8	17	4 (4)	6
14.5	55	14	22	12 (12)	7
13.5	117	35	52	20 (20)	10
12.5	40	11	18	7 (4)	4
11.5	51	11	30	6 (2)	4

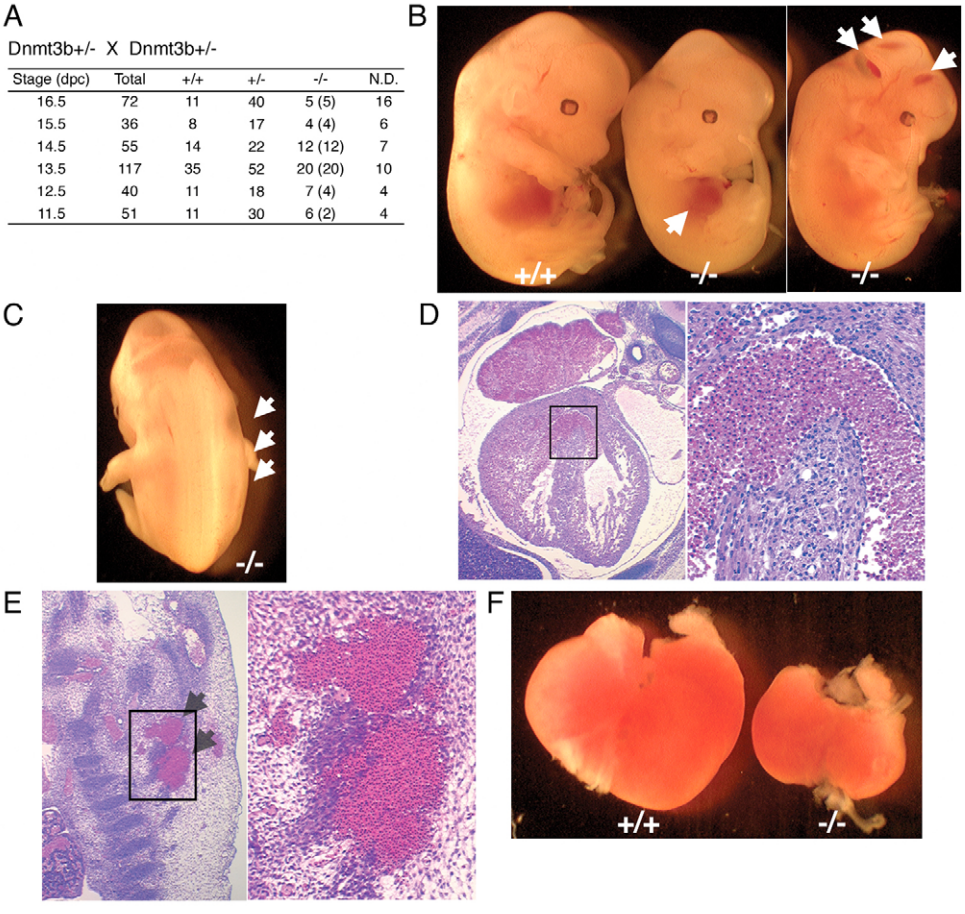

Fig. 4. Developmental defects of *Dnmt3b*$^{-/-}$ embryos. (**A**) Analysis of embryos derived from intercrosses of *Dnmt3b*$^{+/-}$ mice. Numbers in parentheses indicate the number of abnormal embryos. (**B**) Gross morphology of *Dnmt3b*$^{-/-}$ embryos and a wild-type littermate at 13.5 dpc. Some *Dnmt3b*$^{-/-}$ embryos showed a smaller and paler fetal liver than their wild-type littermates, which could be recognized from outside (middle embryo, arrow). Some *Dnmt3b*$^{-/-}$ embryos showed bleeding at the head region (right embryo, arrow). (**C**) Posterior view of the *Dnmt3b*$^{-/-}$ embryo shown in B. Most of the *Dnmt3b*$^{-/-}$ embryo showed subcutaneous edema (arrows) at 13.5 dpc. (**D**) Ventricular septum defect in the heart of a *Dnmt3b*$^{-/-}$ embryo at 14.5 dpc. The right panel shows a higher magnification of the inset shown in D. (**E**) Ectopic hemorrhage at the dorsal root ganglion of a *Dnmt3b*$^{-/-}$ embryo at 12.5 dpc. (**F**) Malformation of the fetal liver in *Dnmt3b*$^{-/-}$ embryos at 13.5 dpc.

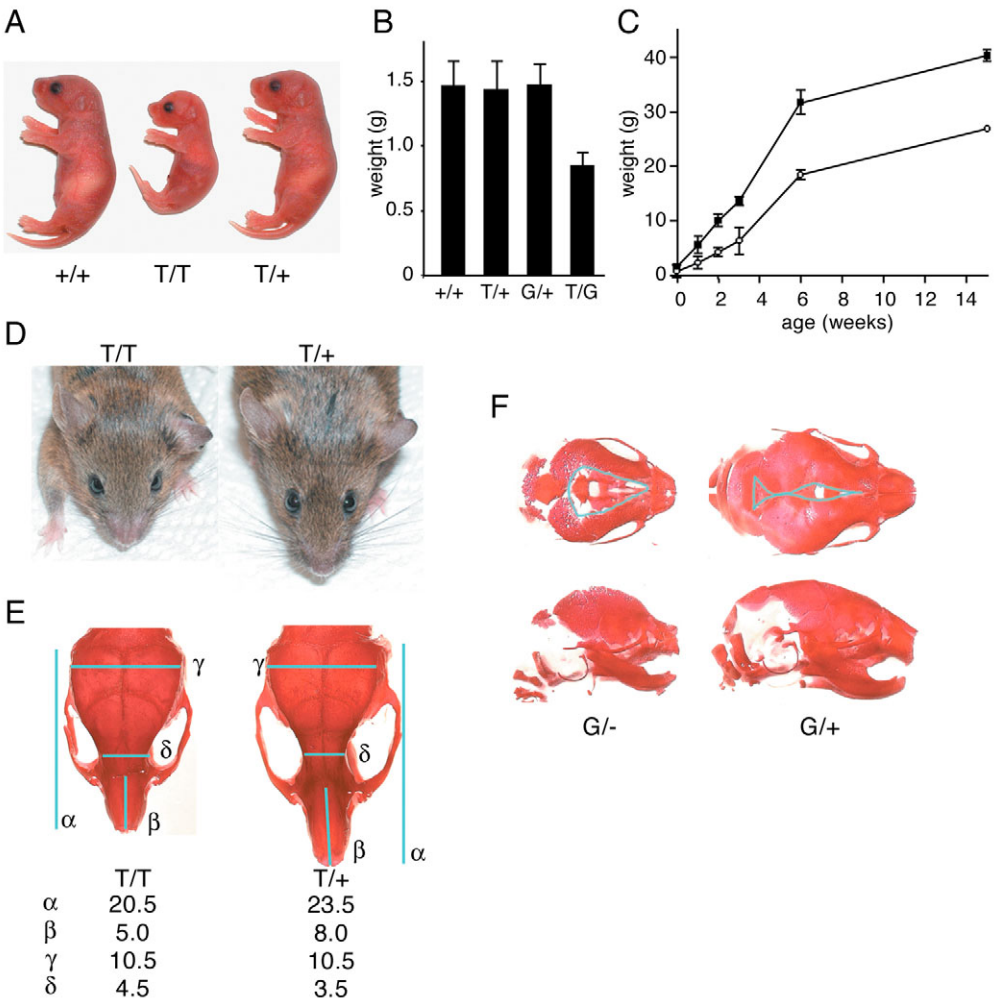

Fig. 5. Gross appearance of ICF mice. (**A**) Gross morphology of wild-type (+/+), T/T and T/+ newborns. The T/T pup was smaller than its wild-type and heterozygous littermates, and lacked a milk spot. (**B**) Average body weight of +/+ (n=6), T/+ (n=5), G/+ (n=7) and T/G (n=5) littermates at birth. Error bars represent the standard error. (**C**) Growth curves of ICF mutant mice (circle) and control mice (black square). Three to 10 mice of each genotype were used for each data point, except for 15-week-old mutant mice of which we analyzed only two. Error bars represent the standard errors. (**D**) Gross appearance of the face of a T/T mouse and a T/+ littermate at P60. (**E**) Dorsal view of bone staining of an adult T/T skull (left) and a T/+ littermate skull (right). The length of the lines of α, β, γ and δ indicated in the panel is shown below. (**F**) Dorsal (upper) and lateral (lower) views of bone staining of a newborn G/– (left) and a G/+ (right) skull. The lines demonstrate the foremen.

were, however, much smaller than those of their littermate controls, and the number of total thymocytes was reduced about 10-fold (Fig. 6B). Analysis of CD4/CD8 subpopulations by flow cytometry revealed that $CD4^+CD8^+$ double-positive (DP) cells were reduced, and the $CD4^-CD8^-$ double-negative (DN) cells were relatively increased (Fig. 6A). The absolute numbers of thymocytes in all of these subpopulations in ICF mice were reduced (Fig. 6B). Analysis of cell death profiles by AnexinV/propidium iodide staining revealed that the majority of P1 ICF mutant thymocytes were dead or dying (+/+, 9%; T/–, 55%; Fig. 6A). These changes were observed in all of the ICF mice we analyzed, including those with T/– (Fig. 6A,B), G/–, T/T and G/G (data not shown) mutations, although the number of total thymocytes varied among different individuals (probably because of the difference in age, which ranges from 24 to 48 hours).

Examination of Hematoxylin/Eosin-stained histology sections showed that the thymus of P1 ICF mice contained a large number of fragmented and condensed nuclei (data not shown). TUNEL staining confirmed that the majority of the thymocytes were undergoing apoptosis in *Dnmt3b* mutant animals (Fig. 6C). No difference in the TUNEL staining of spleen, liver, lung, brain, stomach, gut or kidney was detected between ICF mice and controls (Fig. 6C and data not shown). A dramatic increase in thymocyte apoptosis in P1 ICF mice was also detected by DNA ladder analysis (Fig. 6D). Interestingly, DNA laddering was not observed in the thymus of P0 newborn mice, suggesting that T cell death was induced after birth. These data were also supported by an Annexin V binding analysis, which showed a slight increase in apoptotic cells at the P0 stage and no difference in the number of apoptotic cells obtained from 19 dpc embryos (data not shown). A small degree of DNA laddering was also observed in the spleen of P1 mutant mice, but was not observed in other tissues, including liver, kidney, brain and tail (Fig. 6D and data not shown). Moreover, apoptosis was observed in the thymus of *Dnmt3b* G/G, $p53^{-/-}$ double mutant mice, indicating that the apoptosis is p53 independent (Fig. 6D). These data suggest that Dnmt3b is essential for maintaining the survival of T cells in the thymus of perinatal mice.

DISCUSSION

Our previous studies have shown that inactivation of both *Dnmt3a* and *Dnmt3b* by gene targeting abolishes de novo methylation of the genome during early post-implantation development and causes embryonic lethality at the late gastrula stage (Okano et al., 1999). However, the function of Dnmt3a or Dnmt3b alone in development remains largely unknown. In this study, we showed that mice homozygous for a null mutation of *Dnmt3b* die at the late gastrula stage, whereas mice carrying missense mutations of two human ICF syndrome alleles develop to term. Analysis of *Dnmt3b* mutant mice has revealed that Dnmt3b is essential for the development of the fetal heart, liver and craniofacial structures, and for the survival of T cells at the newborn stage.

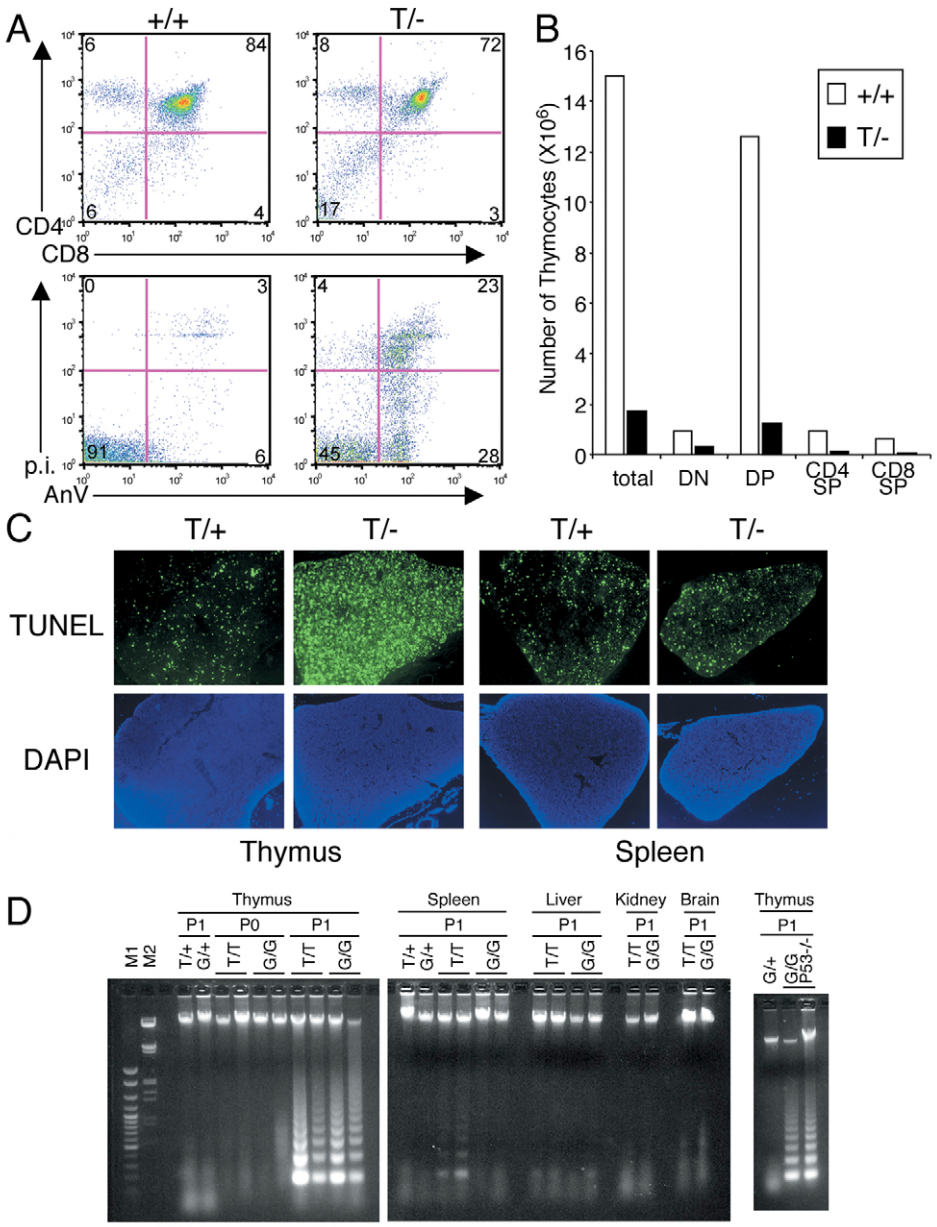

Fig. 6. *Dnmt3b* mutations lead to the apoptosis of thymocytes.
(**A**) Representative FACS profiles showing staining patterns of thymocytes in P1 ICF mice and control mice. Cells were stained with anti-CD4-PE and anti-CD8-FITC for upper panels, and Annexin V-FITC (AnV) and propidium iodide (p.i.) for lower panels. Numbers shown in FACS profiles denote the percentage of cells that fall into each quadrant. (**B**) Absolute numbers of total thymocytes (total), $CD4^{-}CD8^{-}$ double-negative cells (DN), $CD4^{+}CD8^{+}$ double-positive cells (DP), $CD4^{+}$ single-positive cells (CD4 SP), and $CD8^{+}$ single-positive cells (CD8 SP) in a T/– mouse and a wild-type littermate. (**C**) TUNEL staining (upper panels) and DAPI staining (lower panels) of sections of thymus and spleen from a T/– mutant mouse and a T/+ littermate control at P1. (**D**) Fragmentation of DNA extracted from the thymus, spleen, liver, kidney and brain of ICF mutant mice and their littermate controls at P0 or P1. DNA was analyzed by electrophoresis on a 1% agarose gel and stained with ethidium bromide.

ICF mutations result in a partial loss of function of Dnmt3b

ICF syndrome is a rare recessive genetic disorder. Individuals with ICF syndrome can survive to adulthood, but display various defects, most notably immune deficiency and craniofacial abnormalities (Ehrlich, 2003; Wijmenga et al., 2000). Because *Dnmt3b* null mutant mice die during fetal development (Okano et al., 1999), it is believed that individuals with ICF syndrome must have residual DNMT3B activity and that a complete loss of function of DNMT3B is probably incompatible with fetal development in humans. Indeed, most ICF patients carry missense mutations in or near the catalytic domain of DNMT3B and none were homozygous for nonsense alleles (Hansen et al., 1999; Okano et al., 1999; Shirohzu et al., 2002; Wijmenga et al., 2000; Xu et al., 1999), suggesting that the complete loss of function of DNMT3B is lethal. This also implies that most missense mutations in individuals with ICF may not be complete loss-of-function alleles. This notion was supported by the in vitro analysis of six different missense mutations in the catalytic domain of Dnmt3b (Gowher and Jeltsch, 2002). The catalytic activities of the mutant Dnmt3b was shown to be reduced 10- to 50-fold, but was still detectable. However, in vivo studies using cultured mammalian cells expressing Dnmt3b missense mutants characteristic of ICF syndrome failed to detect de novo methylation of episomal DNA (Xu et al., 1999).

In this study, we tested the function of several Dnmt3b mutations in mouse ES cells. We showed that *Dnmt3b* cDNA containing characteristic ICF mutations failed to induce detectable de novo methylation of repetitive sequences after being introduced into mouse ES cells lacking endogenous Dnmt3a and Dnmt3b (Fig. 1E). However, introduction of two of the ICF mutations into the mouse *Dnmt3b* gene did not result in embryonic lethality. The fact that these mice survive to term and adult stages, and show significantly higher levels of genomic methylation than do *Dnmt3b* null embryos, strongly indicates that these ICF mutations are not null, but are hypomorphic alleles. The reason for the difference between the cell culture and in vivo studies is unknown. It is possible that the

introduction of the ICF mutations into the endogenous *Dnmt3b* gene by homologous recombination may allow more precise regulation of Dnmt3b than the introduction of mutant cDNA into ES cells. Dnmt3b may also function more efficiently in whole embryos than in cultured cells.

Developmental defects in *Dnmt3b*-deficient mice

We showed that all *Dnmt3b*$^{-/-}$ mice die during embryonic development between 14.5 and 16.5 dpc as a result of multiple developmental defects, whereas mice expressing point mutations in one or both alleles survive to term. The residual Dnmt3b activity in the ICF mutants is therefore sufficient to allow mutant mice to escape from some of the early developmental defects shown in *Dnmt3b* null embryos.

The embryonic lethality of *Dnmt3b*$^{-/-}$ mice might be caused by several different factors. Dnmt3b may normally repress the expression of genes that control cell growth, and dysregulated activation of these genes may lead to inappropriate growth arrest. We have shown that MEF cells derived from *Dnmt3b*$^{-/-}$ embryos undergo premature senescence (Dodge et al., 2005). It is also possible that the multiple cardiovascular defects observed in *Dnmt3b*$^{-/-}$ mice might lead to fetal death, although the ventricular septal defect alone does not cause embryonic lethality. Dnmt3b is highly expressed in the placental tissues and disruption of Dnmt3b may lead to placental defects and fetal death.

The Dnmt3b hypomorphic mutations (ICF mutations) lead to a partial loss of de novo methyltransferase activity and a decrease in overall methylation of genomic DNA. Most of the Dnmt3b hypomorphic mutants die shortly after birth but the cause of the newborn lethality remains unknown. We found hemorrhages in the head region in some mice, similar to what was observed in *Dnmt3b*$^{-/-}$ embryos. Unlike *Dnmt3b*$^{-/-}$ embryos, no ventricular septum malformation was detected, although some mice showed thickening of the myocardium. Other organs, including brain, lung, liver, kidney, stomach, gut and spleen, appeared to be histologically indistinguishable from their normal littermates. Several knockout mice with global alterations of DNA methylation die shortly after birth. Conditional deletion of Dnmt1 in neural progenitor cells (nestin promoter Cre) leads to perinatal lethality due to respiratory failure in the pups (Fan et al., 2001). Targeted disruption of the *Lsh* gene, which encodes an SNF2 family protein, also causes global hypomethylation and perinatal lethality (Dennis et al., 2001; Geiman and Muegge, 2000). Lsh has been shown to regulate DNA methylation and histone modification (Dennis et al., 2001; Yan et al., 2003a; Yan et al., 2003b). It remains to be determined how Lsh and DNA methylation may regulate developmental processes that are essential for postnatal survival.

Immune defects in Dnmt3b hypomorphic mutants

The two hypomorphic Dnmt3b mutant strains also showed defects in lymphocyte homeostasis. We observed extensive apoptosis of T cells in the thymus of P1 newborn pups. T cell apoptosis appears to start after birth, as the thymocyte profiles were normal in embryonic and newborn (P0) mice. This suggests that de novo DNA methylation plays a crucial role in suppressing T cell apoptosis in the newborn. As Dnmt3b functions primarily as a de novo methyltransferase, and DNA methylation has been shown to regulate the expression of genes including the T cell cytokine genes IL2, IL4 and interferon (INF) (Bruniquel and Schwartz, 2003; Fitzpatrick et al., 1998; Makar et al., 2003), it is possible that alterations in the expression of these genes may trigger cell death.

Recent studies in mice have suggested an important role for DNA methylation in lymphocytes. Mice carrying a hypomorphic Dnmt1 mutation, which causes genome-wide hypomethylation in all tissues, have been shown to develop T cell lymphomas that exhibit chromosomal instabilities (Gaudet et al., 2003). Conditional deletion of Dnmt1 in early double-negative thymocytes leads to impaired survival of TCRαβ+ cells (Lee et al., 2001), suggesting that Dnmt1 is required for the maintenance of mature T cells. The importance of DNA methylation in lymphocyte survival is also suggested by the phenotype of Lsh deficient mice. Targeted deletion of Lsh results in global genomic hypomethylation and perinatal lethality (Dennis et al., 2001; Geiman et al., 2001). Injection of Lsh$^{-/-}$ fetal liver cells into Rag2$^{-/-}$ mice to reconstitute lymphoid development caused a reduction in T cells and B cells compared with controls (Geiman and Muegge, 2000). These results suggest that DNA methylation plays a crucial role in the maintenance and normal function of lymphocytes. The specific target genes regulated by DNA methylation during T cell differentiation, however, remain largely unknown.

Mouse models of ICF syndrome

DNMT3B mutations primarily affect the lymphocytes of individuals with ICF syndrome. Characteristic symptoms include agammaglobulinemia and combined immunodeficiency (Ehrlich, 2003). ICF syndrome patients also exhibit hypomethylation of satellite 2 repeats in the pericentromeric heterochromatin, and rearrangements of chromosomes 1, 9 and 16 via hypomethylated satellite 2 in lymphocytes to form multiradiate chromosomes (Jeanpierre et al., 1993; Xu et al., 1999). It should be noted that chromosomal rearrangements have been observed in bone marrow cells from only one of four patients studied (Fasth et al., 1990; Hulten, 1978; Smeets et al., 1994; Turleau et al., 1989), and have never been detected in fibroblast cells derived from four ICF syndrome patients (Brown et al., 1995; Carpenter et al., 1988; Maraschio et al., 1988; Tiepolo et al., 1979). Facial anomaly is another characteristic symptom afflicting individuals with ICF. However, many of the ICF syndrome symptoms are rare and difficult to study because of a limitation in the number of patients. The development of mouse models are thus of great importance.

In this study, we describe mice with two independent ICF point mutations (A609T and D823G) that show developmental defects including T cell defects, facial anomaly and low body weight, which are common symptoms of human ICF syndrome. In addition, genome-wide hypomethylation was observed in both the ICF-like mice and human patients. In the *Dnmt3b* mutant mice, all repetitive sequences tested were found to be hypomethylated, although the methylation status of single genes has not been analyzed. In ICF patients, hypomethylation of satellite 2, satellite 3, and non-satellite repeats D4Z4 and NBL2 has been observed (Jeanpierre et al., 1993; Kondo et al., 2000; Xu et al., 1999). The striking resemblance of ICF-like *Dnmt3b* mutant mice to individuals with ICF suggests that these mice will serve as good models for understanding the etiology of ICF syndrome and will aid in the identification of target genes that are regulated by DNA methylation during development.

We thank H. Lei and L. Yu for excellent technical assistance. This work was supported by grants CA82389 and GM52106 from the National Institutes of Health (to E.L.). Y.U. is supported by the Japan Society for the Promotion of Science. T.C. is a recipient of a long-term fellowship from the Human Frontier Science Program.

Supplementary material

Supplementary material for this article is available at
http://dev.biologists.org/cgi/content/full/133/6/1183/DC1

References

Bachman, K. E., Rountree, M. R. and Baylin, S. B. (2001). Dnmt3a and Dnmt3b are transcriptional repressors that exhibit unique localization properties to heterochromatin. *J. Biol. Chem.* **276**, 32282-32287.

Brown, D. C., Grace, E., Sumner, A. T., Edmunds, A. T. and Ellis, P. M. (1995). ICF syndrome (immunodeficiency, centromeric instability and facial anomalies): investigation of heterochromatin abnormalities and review of clinical outcome. *Hum. Genet.* **96**, 411-416.

Bruniquel, D. and Schwartz, R. H. (2003). Selective, stable demethylation of the interleukin-2 gene enhances transcription by an active process. *Nat. Immunol.* **4**, 235-240.

Carpenter, N. J., Filipovich, A., Blaese, R. M., Carey, T. L. and Berkel, A. I. (1988). Variable immunodeficiency with abnormal condensation of the heterochromatin of chromosomes 1, 9, and 16. *J. Pediatr.* **112**, 757-760.

Chen, T., Ueda, Y., Xie, S. and Li, E. (2002). A novel Dnmt3a isoform produced from an alternative promoter localizes to euchromatin and its expression correlates with active de novo methylation. *J. Biol. Chem.* **277**, 38746-38754.

Chen, T., Ueda, Y., Dodge, J. E., Wang, Z. and Li, E. (2003). Establishment and maintenance of genomic methylation patterns in mouse embryonic stem cells by Dnmt3a and Dnmt3b. *Mol. Cell. Biol.* **23**, 5594-5605.

Chen, T., Tsujimoto, N. and Li, E. (2004). The PWWP domain of Dnmt3a and Dnmt3b is required for directing DNA methylation to the major satellite repeats at pericentric heterochromatin. *Mol. Cell. Biol.* **24**, 9048-9058.

Dennis, K., Fan, T., Geiman, T., Yan, Q. and Muegge, K. (2001). Lsh, a member of the SNF2 family, is required for genome-wide methylation. *Genes Dev.* **15**, 2940-2944.

Dodge, J. E., Okano, M., Dick, F., Tsujimoto, N., Chen, T., Wang, S., Ueda, Y., Dyson, N. and Li, E. (2005). Inactivation of Dnmt3b in mouse embryonic fibroblasts results in DNA hypomethylation, chromosomal instability, and spontaneous immortalization. *J. Biol. Chem.* **280**, 17986-17991.

Ehrlich, M. (2003). The ICF syndrome, a DNA methyltransferase 3B deficiency and immunodeficiency disease. *Clin. Immunol.* **109**, 17-28.

Fan, G., Beard, C., Chen, R. Z., Csankovszki, G., Sun, Y., Siniaia, M., Biniszkiewicz, D., Bates, B., Lee, P. P., Kuhn, R. et al. (2001). DNA hypomethylation perturbs the function and survival of CNS neurons in postnatal animals. *J. Neurosci.* **21**, 788-797.

Fasth, A., Forestier, E., Holmberg, E., Holmgren, G., Nordenson, I., Soderstrom, T. and Wahlstrom, J. (1990). Fragility of the centromeric region of chromosome 1 associated with combined immunodeficiency in siblings. A recessively inherited entity? *Acta Paediatr. Scand.* **79**, 605-612.

Fitzpatrick, D. R., Shirley, K. M., McDonald, L. E., Bielefeldt-Ohmann, H., Kay, G. F. and Kelso, A. (1998). Distinct methylation of the interferon gamma (IFN-gamma) and interleukin 3 (IL-3) genes in newly activated primary CD8+ T lymphocytes: regional IFN-gamma promoter demethylation and mRNA expression are heritable in CD44 (high) CD8+ T cells. *J. Exp. Med.* **188**, 103-117.

Gaudet, F., Hodgson, J. G., Eden, A., Jackson-Grusby, L., Dausman, J., Gray, J. W., Leonhardt, H. and Jaenisch, R. (2003). Induction of tumors in mice by genomic hypomethylation. *Science* **300**, 489-492.

Geiman, T. M. and Muegge, K. (2000). Lsh, an SNF2/helicase family member, is required for proliferation of mature T lymphocytes. *Proc. Natl. Acad. Sci. USA* **97**, 4772-4777.

Geiman, T. M., Tessarollo, L., Anver, M. R., Kopp, J. B., Ward, J. M. and Muegge, K. (2001). Lsh, a SNF2 family member, is required for normal murine development. *Biochim. Biophys. Acta* **1526**, 211-220.

Georgopoulos, K., Bigby, M., Wang, J. H., Molnar, A., Wu, P., Winandy, S. and Sharpe, A. (1994). The Ikaros gene is required for the development of all lymphoid lineages. *Cell* **79**, 143-156.

Gowher, H. and Jeltsch, A. (2002). Molecular enzymology of the catalytic domains of the Dnmt3a and Dnmt3b DNA methyltransferases. *J. Biol. Chem.* **277**, 20409-20414.

Hansen, R. S., Wijmenga, C., Luo, P., Stanek, A. M., Canfield, T. K., Weemaes, C. M. and Gartler, S. M. (1999). The DNMT3B DNA methyltransferase gene is mutated in the ICF immunodeficiency syndrome. *Proc. Natl. Acad. Sci. USA* **96**, 14412-14417.

Hata, K., Okano, M., Lei, H. and Li, E. (2002). Dnmt3L cooperates with the Dnmt3 family of de novo DNA methyltransferases to establish maternal imprints in mice. *Development* **129**, 1983-1993.

Hulten, M. (1978). Selective somatic pairing and fragility at 1q12 in a boy with common variable immunodeficiency. *Clin. Genet.* **14**, 294.

Jeanpierre, M., Turleau, C., Aurias, A., Prieur, M., Ledeist, F., Fischer, A. and Viegas-Pequignot, E. (1993). An embryonic-like methylation pattern of classical satellite DNA is observed in ICF syndrome. *Hum. Mol. Genet.* **2**, 731-735.

Kaneda, M., Okano, M., Hata, K., Sado, T., Tsujimoto, N., Li, E. and Sasaki, H. (2004). Essential role for de novo DNA methyltransferase Dnmt3a in paternal and maternal imprinting. *Nature* **429**, 900-903.

Kim, G. D., Ni, J., Kelesoglu, N., Roberts, R. J. and Pradhan, S. (2002). Co-operation and communication between the human maintenance and de novo DNA (cytosine-5) methyltransferases. *EMBO J.* **21**, 4183-4195.

Kondo, T., Bobek, M. P., Kuick, R., Lamb, B., Zhu, X., Narayan, A., Bourc'his, D., Viegas-Pequignot, E., Ehrlich, M. and Hanash, S. M. (2000). Whole-genome methylation scan in ICF syndrome: hypomethylation of non-satellite DNA repeats D4Z4 and NBL2. *Hum. Mol. Genet.* **9**, 597-604.

Lakso, M., Pichel, J. G., Gorman, J. R., Sauer, B., Okamoto, Y., Lee, E., Alt, F. W. and Westphal, H. (1996). Efficient in vivo manipulation of mouse genomic sequences at the zygote stage. *Proc. Natl. Acad. Sci. USA* **93**, 5860-5865.

Lee, P. P., Fitzpatrick, D. R., Beard, C., Jessup, H. K., Lehar, S., Makar, K. W., Perez-Melgosa, M., Sweetser, M. T., Schlissel, M. S., Nguyen, S. et al. (2001). A critical role for Dnmt1 and DNA methylation in T cell development, function, and survival. *Immunity* **15**, 763-774.

Lei, H., Oh, S. P., Okano, M., Juttermann, R., Goss, K. A., Jaenisch, R. and Li, E. (1996). De novo DNA cytosine methyltransferase activities in mouse embryonic stem cells. *Development* **122**, 3195-3205.

Li, E., Bestor, T. H. and Jaenisch, R. (1992). Targeted mutation of the DNA methyltransferase gene results in embryonic lethality. *Cell* **69**, 915-926.

Makar, K. W., Perez-Melgosa, M., Shnyreva, M., Weaver, W. M., Fitzpatrick, D. R. and Wilson, C. B. (2003). Active recruitment of DNA methyltransferases regulates interleukin 4 in thymocytes and T cells. *Nat. Immunol.* **4**, 1183-1190.

Maraschio, P., Zuffardi, O., Dalla Fior, T. and Tiepolo, L. (1988). Immunodeficiency, centromeric heterochromatin instability of chromosomes 1, 9, and 16, and facial anomalies: the ICF syndrome. *J. Med. Genet.* **25**, 173-180.

Okano, M., Xie, S. and Li, E. (1998). Cloning and characterization of a family of novel mammalian DNA (cytosine-5) methyltransferases. *Nat. Genet.* **19**, 219-220.

Okano, M., Bell, D. W., Haber, D. A. and Li, E. (1999). DNA methyltransferases Dnmt3a and Dnmt3b are essential for de novo methylation and mammalian development. *Cell* **99**, 247-257.

Shirohzu, H., Kubota, T., Kumazawa, A., Sado, T., Chijiwa, T., Inagaki, K., Suetake, I., Tajima, S., Wakui, K., Miki, Y. et al. (2002). Three novel DNMT3B mutations in Japanese patients with ICF syndrome. *Am. J. Med. Genet.* **112**, 31-37.

Smeets, D. F., Moog, U., Weemaes, C. M., Vaes-Peeters, G., Merkx, G. F., Niehof, J. P. and Hamers, G. (1994). ICF syndrome: a new case and review of the literature. *Hum. Genet.* **94**, 240-246.

Tiepolo, L., Maraschio, P., Gimelli, G., Cuoco, C., Gargani, G. F. and Romano, C. (1979). Multibranched chromosomes 1, 9, and 16 in a patient with combined IgA and IgE deficiency. *Hum. Genet.* **51**, 127-137.

Turleau, C., Cabanis, M. O., Girault, D., Ledeist, F., Mettey, R., Puissant, H., Prieur, M. and de Grouchy, J. (1989). Multibranched chromosomes in the ICF syndrome: immunodeficiency, centromeric instability, and facial anomalies. *Am. J. Med. Genet.* **32**, 420-424.

Webb, S., Brown, N. A. and Anderson, R. H. (1998). Formation of the atrioventricular septal structures in the normal mouse. *Circ. Res.* **82**, 645-656.

Wijmenga, C., Hansen, R. S., Gimelli, G., Bjorck, E. J., Davies, E. G., Valentine, D., Belohradsky, B. H., van Dongen, J. J., Smeets, D. F., van den Heuvel, L. P. et al. (2000). Genetic variation in ICF syndrome: evidence for genetic heterogeneity. *Hum. Mutat.* **16**, 509-517.

Winandy, S., Wu, P. and Georgopoulos, K. (1995). A dominant mutation in the Ikaros gene leads to rapid development of leukemia and lymphoma. *Cell* **83**, 289-299.

Xie, S., Wang, Z., Okano, M., Nogami, M., Li, Y., He, W. W., Okumura, K. and Li, E. (1999). Cloning, expression and chromosome locations of the human DNMT3 gene family. *Gene* **236**, 87-95.

Xu, G. L., Bestor, T. H., Bourc'his, D., Hsieh, C. L., Tommerup, N., Bugge, M., Hulten, M., Qu, X., Russo, J. J. and Viegas-Pequignot, E. (1999). Chromosome instability and immunodeficiency syndrome caused by mutations in a DNA methyltransferase gene. *Nature* **402**, 187-191.

Yan, Q., Cho, E., Lockett, S. and Muegge, K. (2003a). Association of Lsh, a regulator of DNA methylation, with pericentromeric heterochromatin is dependent on intact heterochromatin. *Mol. Cell. Biol.* **23**, 8416-8428.

Yan, Q., Huang, J., Fan, T., Zhu, H. and Muegge, K. (2003b). Lsh, a modulator of CpG methylation, is crucial for normal histone methylation. *EMBO J.* **22**, 5154-5162.